Journal of Nano- and Electronic Physics
Vol. **14** No 4, 04002(5pp) (2022)

Журнал нано- та електронної фізики
Том **14** № 4, 04002(5cc) (2022)

Structural, Optical and Magnetic Properties of $Cd_{1-x}Mn_xS$ Nanocrystalline Thin Films at Room Temperature

Ashok E. Mali*, Anil S. Gaikwad, Sanjay V. Borse, Rajendra R. Ahire

[1] *Department of Physics, SPDM College, 425405 Shirpur, Dist. Dhule (MS), India*
[2] *Department of Physics, SSVPS College, 425406 Shindkheda, Dist. Dhule (MS), India*
[3] *Department of Physics, SG Patil College, 424304 Sakri, Dist. Dhule (MS), India*

(Received 24 June 2022; revised manuscript received 11 August 2022; published online 25 August 2022)

$Cd_{1-x}Mn_xS$ (x = 0.0, 0.2, 0.4, 0.6, 0.8, and 1.0) films were prepared using a low-cost chemical bath deposition (CBD) technique onto the glass substrate. Films were obtained at an optimized bath temperature of 80 °C and pH of 11. In the current study, we investigated the structural, optical, and magnetic properties of the as-deposited thin films. The X-ray diffraction (XRD) result confirmed that the nanocrystalline structure has a high aspect ratio compared to CdMnS films. XRD suggests hexagonal wurtzite and cubic structures with growth orientation along the (002) direction. The lattice parameter '*a*' decreased from 4.126 to 4.003 Å. The same trend in the lattice parameter '*c*' with x was observed (5.263 to 5.200 Å). The optical properties of as-deposited $Cd_{1-x}Mn_xS$ nanocrystalline films were studied at room temperature using a UV-visible spectrophotometer. The optical band gap is found to be enhanced with Mn^{2+} composition. Group II-VI-based diluted magnetic semiconductors (DMS) show distinct magnetic phases at low and room temperatures. The magnetic behavior and susceptibility studies were carried out using a superconducting quantum interference device (SQUID) on a vibrating sample magnetometer (VSM) in the range of dc magnetic field of 0-40 kOe at room temperature.

Keywords: CdMnS films, Mn^{2+} magnetic ions, DMS, Lattice parameters, Magnetic measurements.

DOI: 10.21272/jnep.14(4).04002 PACS numbers: 68.55.ag, 78.66.Hf, 75.30.cr, 85.25.Dq, 75.70.Ak

1. INTRODUCTION

The doping of transition metals into II-VI, III-V, and IV-VI semiconductors leads to a new class of semiconductors known as diluted magnetic semiconductors (DMSs) [1]. DMSs are alloys with magnetic ions diluted in a nonmagnetic semiconductor. Because of tunable bandgap and lattice parameters, the Mn-based DMSs can be grown over a wider composition range than Fe and Co-based DMSs. The tunability of lattice parameters and bandgap parameters with different concentrations of Mn is the unique property of DMSs and is excellent in the fabrication of quantum well devices and superlattices [2, 3]. Recently, CdS-based DMSs have attracted more attention due to their immense application such as magneto-optical devices.

CdS (bandgap of 2.42 eV at 300 K) is a direct bandgap II-VI semiconductor family. Doping of manganese into CdS can tailor the optical and luminescence properties. Recently, II-VI semiconductor materials have shown room-temperature ferromagnetism. The room-temperature ferromagnetism in CdS offers great development in the fabrication of magneto-optical and spintronics devices. DMS is considered an ideal semiconductor for spintronics, which is a rapidly growing field in physics, intensively studying the spin-dependent phenomena applied to modern electronic devices. Manganese (Mn) doped CdMnS is one of the important DMS materials considered to be optoelectronic, nonlinear optical, fast optical switching, and memory devices [4].

DMSs are semiconducting alloys formed by randomly replacing a fraction of cations with magnetic ions (Mn^{2+} in CdS to form $Cd_{1-x}Mn_xS$). The presence of manganese in a semiconductor alloy leads to an exchange interaction between *s-p* band electrons and manganese *d* electrons [5-9].

2. EXPERIMENTAL DETAILS

$Cd_{1-x}Mn_xS$ nanocrystalline thin films with different compositions of Mn, for x = 0.0, 0.2, 0.4, 0.6, 0.8, and 1.0 were prepared onto the chemically cleaned glass slides by using the chemical bath deposition (CBD) technique. A freshly synthesized solution of cadmium chloride (1 M), manganese chloride (1 M), and thiourea (1 M) in their stoichiometric proportion was taken in a glass beaker of 100 ml in capacity. Ammonia was added to the reaction container as the complexing agent. The glass substrate was cleaned and placed vertically tilted in the reaction container. For each of the compositional parameters '*x*', the film stoichiometry was maintained by adjusting the ion concentration volume of the used reactants. To achieve a good quality of the films, the complexing agent, deposition time, temperature and pH of the solution were optimized. Best quality films were obtained after a great deal of trial and error. The prepared $Cd_{1-x}Mn_xS$ films exhibit yellowish to a yellow-brownish color with variation in the compositional parameter '*x*'.

3. RESULTS AND DISCUSSION

3.1 UV-Visible Spectroscopy Analysis

The optical absorption spectra were recorded by a spectrophotometer in the wavelength range of 300-900 nm. The optical absorption spectra of $Cd_{1-x}Mn_xS$ thin films were utilized to determine the optical band

* aemalispdm@gmail.com

gap (E_g) using the Tauc plot method given by the following formula:

$$(\alpha h\vartheta) = A(h\vartheta - E_g)n,$$

where α is the absorption coefficient, A is a constant, $h\vartheta$ is the photon energy, and $n = 1/2$ for direct bandgap material.

It is observed that the optical band gap values have been enhanced with the compositional parameter x. Fig. 1 shows a plot of the optical band gap as a function of the composition 'x'. With an increase in the compositional parameter x, the strain was developed by Mn^{2+} ion in the lattice structure and therefore it becomes highly distorted that causes the optical band gap to increase. This enhancement in the band gap value is consistent with the previous literature [10]. A systematic increase in the value of E_g with Mn^{2+} concentration can be envisaged. The increase in a bandgap is related to quantum confinement effects.

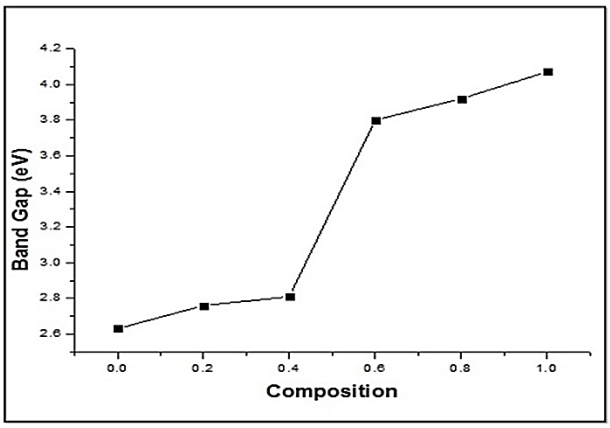

Fig. 1 – Optical bandgap as a function of composition

3.2 XRD Analysis

The XRD spectra of $Cd_{1-x}Mn_xS$ films are shown in Fig. 2. The diffractograms clearly show that the obtained films are polycrystalline with both hexagonal and cubic wurtzite structures with preferential growth along the (002) direction.

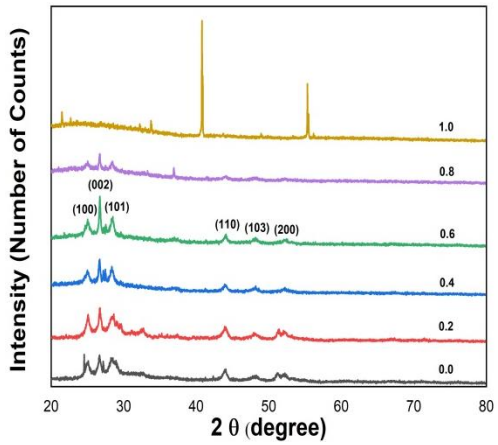

Fig. 2 – XRD spectra of the obtained samples

Peaks at diffraction angles of 25.02, 26.72, 28.51, 44.11, 48.20, and 52.45° correspond to the (100), (002), (101), (110), (103) and (200) planes, respectively, of the hexagonal wurtzite $Cd_{1-x}Mn_xS$ thin films compared with the standard JCPDS card (numbers 772306 for CdS and 894953 for MnS). Increased Mn composition in $Cd_{1-x}Mn_xS$ leads to positional shifts of diffraction peaks to higher scattering angles which may result from a reduction of the lattice parameters by substitution of Cd^{2+} ions with the smaller radius Mn^{2+} ions [11]. It has been found that the crystal structure of CBD prepared $Cd_{1-x}Mn_xS$ thin films was wurtzite hexagonal structures for x varied from 0.0 to 0.8 and was not observed for $x = 1.0$. The lattice parameters 'a' and 'c' of the hexagonal structure are calculated using the following equation [12]:

$$1/d^2 = (4/3)\,[(h^2 + k^2 + hk)/a^2] + (l^2/c^2),$$

where d is the lattice spacing, h, k, l are Miller indices.

Table 1 shows the lattice parameters, c/a ratio, u-parameter, and Cd-S bond lengths. The lattice parameter 'a' decreased from 4.1263 to 4.0030 with an increase in Mn concentration (x) in the coating solution from 0.0 to 1.0. Similar changes in the parameter 'c' have been observed (5.2639 to 5.2001). A decrease in the lattice parameters is attributed to the smaller atomic size of Mn ($r_{mn} = 0.80$ Å) than that of Cd ($r_{cd} = 0.92$ Å) [13-15]. The linear behavior of both lattice parameters 'a' and 'c' with Mn^{2+} composition has been observed which follows Vegard's law [16-18]. Thus, the XRD pattern shows that contraction of the lattice parameters confirming the incorporation of Mn^{2+} ($x \geq 0.8$) resulted in the formation of separate phases of both CdS and MnS. The average grain size is enhanced from 22 to 179 nm as the composition x increases from 0.0 to 1.0. A similar type of behavior was reported in $Cd_{1-x}Mn_xS$ thin films deposited by the CBD technique [19].

The c/a ratio of incorporation of Mn into CdS is observed to be constant and is in good agreement with the standard value (1.27). A significant increase in the c/a ratio is observed with increased Mn doping. The 'u' parameter is calculated using the following relation:

$$u = (a^2 + 3c^2) + 0.25.$$

A slight change in the calculated 'u' parameter indicates the incorporation of Mn atom in CdS crystal. Cd-S bond lengths are calculated using the following formula:

$$L = [(a^2/3) + (1/2 - u)^2 z^2]^{1/2}.$$

Diminutive decrement is observed in the Cd-S bond length with doping concentration enhancement. The measured bond length of Cd-S in deposited CdMnS materials is 2.3941 Å and is observed well with previous literature [20].

3.3 FESEM Analysis

The surface morphology of $Cd_{1-x}Mn_xS$ thin films deposited at $x = 0.2$ was investigated by using FESEM analysis. Fig. 3 shows the FESEM micrograph of CdMnS films having flower-like uniform surface morphologies. Pure CdS has a nano-sheet-like structure

Table 1 – Lattice parameters, *c*/*a* ratio, *u*-parameter, and Cd-S bond length of the prepared samples

Composition	Lattice parameters (Å)		*c*/*a* ratio	*u* parameter	Bond length (Å)
	a	*c*			
0.0	4.1263	5.2639	1.2756	0.4548	2.3941
0.2	4.1170	5.2540	1.2761	0.4546	2.3888
0.4	4.1185	5.2529	1.2754	0.4549	2.3895
0.6	4.1165	5.2500	1.2753	0.4549	2.3884
0.8	4.1137	5.2709	1.2811	0.4530	2.3878
1.0	4.003	5.2001	1.2990	0.4475	–

Fig. 3 – FESEM micrograph of $Cd_{1-x}Mn_xS$ thin films deposited at $x = 0.2$

and turns into a nano flower-like structure by the addition of Mn^{2+} ions into the CdS structure.The nanocrystalline behavior of thin films is also supported by grain size estimated from XRD data.

3.4 Magnetic Properties

- **VSM Studies**

Magnetization measurements were conducted using a 7T superconducting quantum interference device (SQUID) on a vibrating sample magnetometer (VSM). Fig. 4 shows a variation of magnetization as a function of magnetic field for $Cd_{1-x}Mn_xS$ thin films at various compositions. The magnetic properties of as-deposited $Cd_{1-x}Mn_xS$ thin films have been studied as a function of Mn^{2+} ion concentration from these VSM images.

It is clear from these VSM images, that the hysteresis loop is symmetric concerning zero magnetic fields. From these hysteresis loops, various magnetic properties of the samples were calculated. The calculated values of various magnetic properties are tabulated in Table 2. The saturation magnetization (M_s) increases with the Mn^{2+} ion concentration of the films. An increase in M_s was probably caused by an increase in the number of electrons which induced more efficient ferromagnetic coupling between doped Mn^{2+} ions. The free carrier concentration is induced in Mn^{2+} ion-doped CdS films by substitutions of Mn^{2+} ion into the CdS lattices that will lead to room temperature ferromagnetism in the samples [21-23]. Also, the magnetic coercivity (H_c) increases with increasing the Mn^{2+} ion concentration. The increase in H_c with Mn^{2+} ion concentration may be due to the ferromagnetic behavior of $Cd_{1-x}Mn_xS$ thin films.

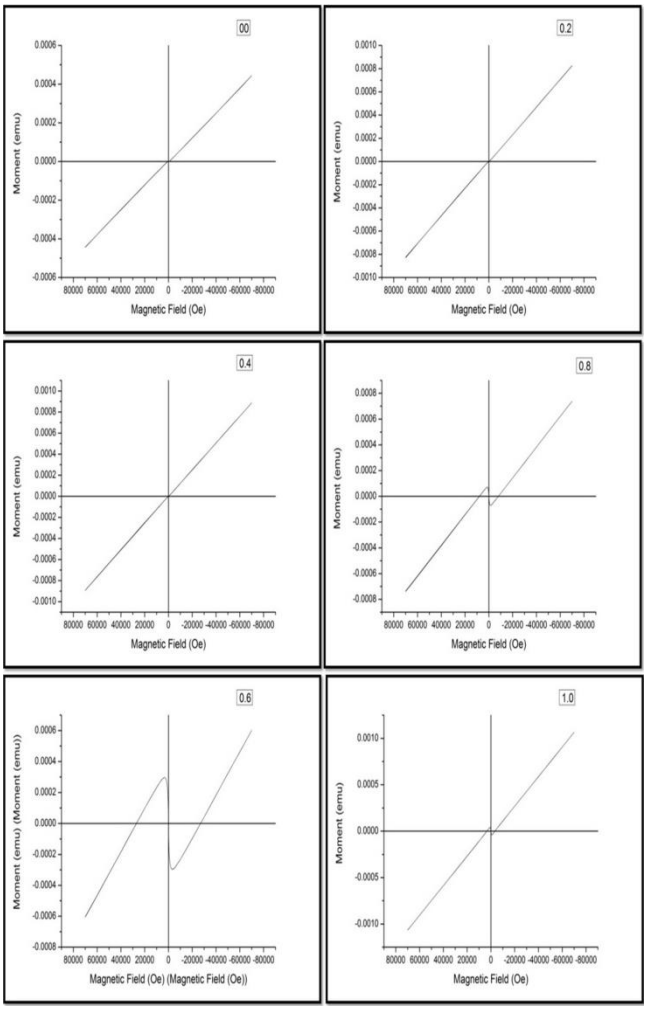

Fig. 4 – Variation of magnetization as a function of magnetic field for $Cd_{1-x}Mn_xS$ thin films versus composition

- **Magnetic Susceptibility Studies**

The magnetization data from SQUID-VSM measurement showed the ferromagnetic-like behavior at room temperature for all $Cd_{1-x}Mn_xS$ thin films. The magnetic susceptibility studies were conducted at room temperature with a magnetic field of 40 kOe. Fig. 5 shows the variation of magnetic susceptibility with Mn^{2+} ion concentration. It is clear from the figure that, susceptibility varies nonlinearly with increasing the value of Mn^{2+} ion concentration. The slope of the susceptibility χ_m versus the composition x curve at lower concentration ($x < 0.4$) is more compared with the slope at higher concentrations ($x > 0.4$). In DMSs, the *sp-d* interactions are responsible for magnetism.

Table 2 – Various magnetic parameters calculated from VSM images

Mn^{2+} composition 'x'	Magnetic saturation M_s (emu)	Magnetic coercivity H_c (Oe)	Magnetic retentivity M_R (emu)
0.0	46.50×10^{-5}	512	4.130×10^{-7}
0.2	84.65×10^{-5}	101	5.369×10^{-7}
0.4	85.00×10^{-5}	486.6	4.80×10^{-7}
0.6	62.25×10^{-5}	27856	6.64×10^{-7}
0.8	75.60×10^{-5}	8009	2.260×10^{-7}
1.0	110.12×10^{-5}	3441	1.2×10^{-7}

The nature of magnetism in $Cd_{1-x}Mn_xS$ thin films may be understood as follows. In CdMnS thin films, each Mn^{2+} ion has a total spin of $s = 5/2$ originating from half-filled 3*d* states, and Mn^{2+} spins are coupled by a short-range anti-ferromagnetic interaction [24]. The results are consistent with those of $Cd_{1-x}Mn_xS$ powder studied by magnetic susceptibility balance mark-1 (MSB-1). The nonlinear variation of χ_m with composition x for $Cd_{1-x}Mn_xS$ thin films may be explained as follows. At lower concentrations of the Mn^{2+} content, *sp* electrons with a spin opposite to the spin of atoms in the CdS lattice interact with the *d* electrons of the Mn^{2+} ion, which causes a decrease in susceptibility. At higher concentrations of Mn^{2+}, the *d-d* exchange interaction between Mn atoms dominates over the *sp-d* exchange interaction resulting in an abrupt increase in susceptibility.

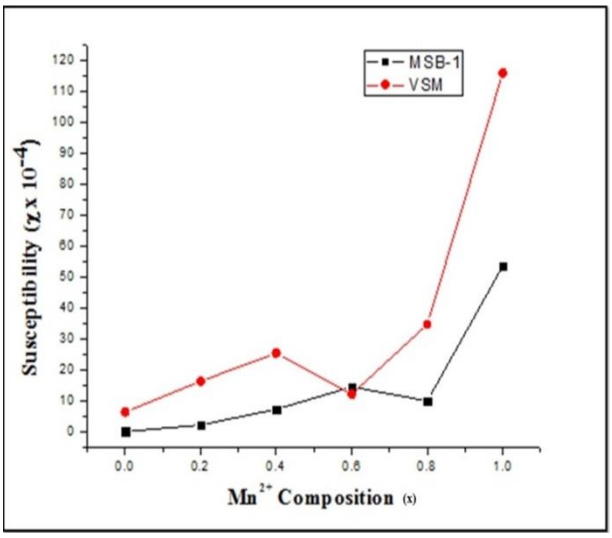

Fig. 5 – Comparison of susceptibility values obtained by MSB-1 and SQUID VSM

The χ_m values estimated from SQUID-VSM measurement data are in good agreement with values obtained from magnetic susceptibility balance (MSB) mark-1. The magnetic susceptibility is determined by MSB-1 using the relation given below:

$$\chi_m = \chi_g \, x \, MW,$$

where MW is the molecular weight of the substance. The mass susceptibility (χ_g) is calculated using the formula

$$\chi_g = (C \times l \times (R - R_0)) / (10^9 \times m),$$

where l is the sample length, m is the sample mass, R is the reading of tube plus sample, R_0 is the empty tube reading and C is the calibration constant for the used balance. The magnetic behavior of Mn^{2+} doped CdS thin films confirm that the Mn^{2+} content in the CdS structure has induced ferromagnetic properties. Moreover, the magnetization increased due to the induced ferromagnetic coupling between doped Mn^{2+} ions. Since CdS is doped with Mn^{2+}, the thin film shows ferromagnetic nature, and these films can have applications in spintronics.

4. CONCLUSIONS

In conclusion, we have prepared superior quality $Cd_{1-x}Mn_xS$ thin films through a simple chemical bath deposition route with $CdCl_2$, H_2O, $MnCl_2$, $2H_2O$, $(NH_4)_2S$ as precursors. The optimum conditions of bath temperature of 80 °C and pH ~ 11 yielded good adherence and surface coverage with $Cd_{1-x}Mn_xS$ thin films. XRD studies revealed that $Cd_{1-x}Mn_xS$ films have a hexagonal wurtzite structure with growth orientation along the (002) direction. Grain sizes were seen to be in the range of 22 to 179 nm. The variation in the lattice parameters showed Vegard's behavior and confirmed the incorporation of Mn^{2+} ions into CdS crystal. The optical study revealed an increase in the band gap (E_g) of the films. The saturation magnetization and magnetic coercivity increased with an increase in Mn^{2+} composition, and room temperature ferromagnetism was obtained. Thin films exhibited room temperature ferromagnetic properties by variation of magnetization as a function of the applied magnetic field. The magnetic susceptibility of $Cd_{1-x}Mn_xS$ thin films varied nonlinearly with an increase in the Mn^{2+} composition. The magnetic susceptibility obtained from SQUID-VSM data is in good agreement with the estimates obtained from MSB mark 1. The spin-exchange interaction between semiconductor charge carriers and Mn^{2+} ions (*sp-d* exchange interaction) modify $Cd_{1-x}Mn_xS$ thin film properties making them useful for spintronics, non-volatile memories, magneto-optical devices, etc.

ACKNOWLEDGEMENTS

This work was supported by the University Grants Commission (UGC, WRO), Pune, India under a minor research project scheme (File No. 47-1066/14 (WRO), dated 08/01/2016). The authors are also thankful to the UGC-DAE Consortium for Scientific Research (formerly known as IUC-DAEF), Indore, India, for providing the necessary characterization facilities.

AUTHOR CONTRIBUTIONS

Ashok E. Mali and Anil S. Gaikwad contributed equally to the manuscript preparation, design of the experimental setup, measurements and analysis, while Sanjay V. Borse and Rajendra R. Ahire contributed to the composition of the manuscript and result analysis.

REFERENCES

1. J.K. Furdyna, *J. Appl. Phys.* **64**, R29 (1988).
2. B.T. Jonker, X. Liu, W.C. Chou, A. Petrou, J. Warnock, J.J. Krebs, G.A. Prinz, *J. Appl. Phys.* **69**, 6097 (1991).
3. W.C. Chou, A. Petrou, J. Warnock, B.T. Jonker, *Phys. Rev. Lett.* 67, 3820 (1991).
4. R.J. Bandaranayake, J.Y. Lin, H.X. Jiang, C.M. Sorensen, *J. Magn. Magn. Mater.* **169** No 3, 289 (1997).
5. G. Murali, D.A. Reddy, G. Giribabu, R.P. Vijayalakshmi, R. Venugopal, *J. Alloy. Compd.* **581**, 849 (2013).
6. K. Karthik, S. Pushpa, M.M. Naik, M. Vinuth, *Mater. Res. Innov.* **24** No 2, 82 (2020).
7. R. Murugesan, S. Sivakumar, K. Karthik, P. Anandan, M. Haris, *Curr. Appl. Phys.* **19** No 10, 1136 (2019).
8. A.E. Mali, A.S. Gaikwad, S.V. Borse, R.R. Ahire, *J. Nano-Electron. Phys.* **13** No 1, 01004 (2021).
9. Q. Wang, Z. Xu, L. Yue, W. Chen, *Opt. Mater.* **27** No 3, 453 (2004).
10. S.M.H. Al-Jawad, *Int. J. Appl. Innov. Eng. Manag.* **3** No 2, 329 (2014).
11. R. Mariappan, M. Ragavendar, V. Ponnuswamy, *J. Alloy. Compd.* **509** No 27, 7337 (2011).
12. Y.Y. Xi, T.L. Cheung, D.H. Ng, *Mater. Lett.* **62** No 1, 128 (2008).
13. V.D. Mote, J.S. Dargad, Y. Purushotham, B.N. Dole, *Ceram. Int.* **41** No 10, 15153 (2015).
14. S. Aksu, E. Bacaksiz, M. Parlak, S. Yilmaz, I. Polat, M. Altunbaş, M. Türksoy, R. Topkaya, K. Özdoğane, *Mater. Chem. Phys.* **130** No 1-2, 340 (2011).
15. C.T. Tsai, S.H. Chain, D.S. Chu, W.C. Chou, *Phys. Rev. B.* **54**, 11555 (1996).
16. M. Girish, R. Sivakumar, C. Sanjeeviraja, *Optic* **227**, 166088 (2021).
17. J.M. Pawlikowski, *Diluted Magnetic Semiconductor* (World Scientific Publishing Com. Pvt. Lt. Singapore, 1991).
18. M. Boshta, S.A. Gad, A.M. Abo El-Soud, M.Z. Mostafa, *J. Ovonic Res.* **4** No 6, 175 (2008).
19. S.V. Borse, S.D. Chavan, R. Sharma, *J. Alloy Compd.* **436** No 1-2, 407 (2007).
20. The Materials Project. Materials Data on CdS by Materials Project. United States: N. p., (2020).
21. S. Kumar, S. Kumar, S. Jain, N.K. Verma, *Appl. Nanosci.* **2** No 2, 127 (2012).
22. Y. Gao, L. Sun, P. Chen, W. Zhang, *Appl. Phys. A* **103** No 1, 97 (2011).
23. Z. Yang, D. Gao, Z. Zhu, J. Zhang, Z. Shi, Z. Zhang, D. Xue, *Nanoscale Res. Lett.* **8**, 17 (2013).
24. K. Veerabrahamam, D. Raja Reddy, B.K. Reddy, *Spectrochim. Acta A* **60**, 741 (2004).

Структурні, оптичні та магнітні властивості нанокристалічних тонких плівок $Cd_{1-x}Mn_xS$ при кімнатній температурі

Ashok E. Mali, Anil S. Gaikwad, Sanjay V. Borse, Rajendra R. Ahire

[1] *Department of Physics, SPDM College, 425405 Shirpur, Dist. Dhule (MS), India*
[2] *Department of Physics, SSVPS College, 425406 Shindkheda, Dist. Dhule (MS), India*
[3] *Department of Physics, SG Patil College, 424304 Sakri, Dist. Dhule (MS), India*

Плівки $Cd_{1-x}Mn_xS$ (x = 0,0; 0,2; 0,4; 0,6; 0,8 та 1,0) були виготовлені за допомогою недорогої техніки хімічного осадження з ванни (CBD) на скляну підкладку. Плівки були отримані при оптимізованій температурі ванни 80 °C і pH 11. У поточному дослідженні ми вивчали структурні, оптичні та магнітні властивості осаджених тонких плівок. Рентгенівська дифракція (XRD) підтвердила, що нанокристалічна структура має більшу величину c/a порівняно з плівками CdMnS. XRD свідчить про гексагональні та кубічні структури вюрциту з орієнтацією росту вздовж напряму (002). Параметр решітки a зменшився з 4,126 до 4,003 Å. Спостерігалася та сама тенденція і для параметру решітки c з величиною x від 5,263 до 5,200 Å. Оптичні властивості осаджених нанокристалічних плівок $Cd_{1-x}Mn_xS$ досліджували при кімнатній температурі за допомогою УФ-видимого спектрофотометра. Виявлено, що оптична заборонена зона збільшується з додаванням Mn^{2+}. Розбавлені магнітні напівпровідники (DMS) II-VI груп демонструють чіткі магнітні фази при низьких і кімнатних температурах. Дослідження магнітної поведінки та сприйнятливості проводили за допомогою надпровідного квантового інтерференційного пристрою (SQUID) на магнітометрі з вібруючим зразком (VSM) в діапазоні постійного магнітного поля 0-40 кЕ при кімнатній температурі.

Ключові слова: Плівки CdMnS, Магнітні іони Mn^{2+}, DMS, Параметри ґратки, Магнітні вимірювання.